Early detection of the *PAX3-FOXO1* fusion gene in circulating tumor-derived DNA in a case of alveolar rhabdomyosarcoma

Minenori Eguchi-Ishimae,[1] Mari Tezuka,[1] Tomoki Kokeguchi,[2] Kozo Nagai,[1] Kyoko Moritani,[1] Sachiko Yonezawa,[3] Hisamichi Tauchi,[1] Kiriko Tokuda,[4] Yasushi Ishida,[4] Eiichi Ishii,[1] and Mariko Eguchi[1]

[1]Department of Pediatrics, Ehime University Graduate School of Medicine, Toon, Ehime, Japan

[2]Division of Pediatrics, Ehime Prefectural Niihama Hospital

[3]Division of Pediatrics, Matsuyama Red Cross Hospital

[4]Division of Pediatrics/Pediatric Medical Center, Ehime Prefectural Central Hospital

Running head: *PAX3-FOXO1* in circulating cell-free DNA

Correspondence: Dr. Mariko Eguchi,

Department of Pediatrics, Ehime University Graduate School of Medicine, Shitsukawa, Toon, Ehime 791-0295, Japan

Phone: +81-89-960-5320; Fax: +81-89-960-5941

E-mail: maeguchi@m.ehime-u.ac.jp

Abstract

Cell-free DNA (cfDNA), which are small DNA fragments in blood derived from dead cells including tumor cells, could serve as useful biomarkers and provide valuable genetic information about the tumors. cfDNA is now used for the genetic analysis of several types of cancers, as a surrogate for tumor biopsy, designated as 'liquid biopsy'. Rhabdomyosarcoma, the most frequent soft tissue tumor in childhood, can arise in any part of the body, and radiological imaging is the only available method for estimating the tumor burden, because no useful specific biological markers are present in the blood. Because tumor volume is one of the determinants of treatment response and outcome, early detection at diagnosis as well as relapse is essential for improving the treatment outcome. A 15-year-old male patient was diagnosed with alveolar rhabdomyosarcoma of prostate origin with bone marrow invasion. The *PAX3-FOXO1* fusion was identified in the tumor cells in the bone marrow. After the diagnosis, cfDNA was serially collected to detect the *PAX3-FOXO1* fusion sequence as a tumor marker. cfDNA could be an appropriate source for detecting the fusion gene; assays using cfDNA have proved to be useful for the early detection of tumor progression/recurrence. Additionally, the fusion gene dosage estimated by quantitative PCR reflected the tumor volume during the course of the treatment. We suggest that for fusion gene-positive rhabdomyosarcomas, and other soft tissue tumors, the fusion sequence should be used for monitoring the tumor burden in the body, to determine the diagnosis and treatment options for the patients.

Keywords: rhabdomyosarcoma, *PAX3-FOXO1*, cell-free DNA, liquid biopsy

1 INTRODUCTION

Small fragments of DNA derived from dead cells are ubiquitously present in circulating blood; they are known as cell-free DNA (cfDNA). Despite their extremely short half-life,[1] cfDNA could provide vital clues regarding the disease state in many pathological conditions. The cfDNA derived from tumor cells is called circulating tumor DNA (ctDNA), and the amount of ctDNA in blood may correlate well with the tumor burden in the whole body, and also provide valuable information about the genetic variations observed in tumor cells.[2-4] Because ctDNA is derived from dead and processed tumor cells,[5] it could represent the entire set of genetic alterations harbored by the tumor cells, and could serve as a useful, easily available tumor biomarker. Presence of tumor-specific gene mutation(s), such as the oncogenic *KRAS* mutations, could directly indicate the presence of tumors somewhere in the body. In addition, the detection of tumor-specific mutations in ctDNA could be a useful indicator for characterizing the genetic makeup of the tumor cells, and in categorizing, staging, and predicting the treatment outcomes. The term 'liquid biopsy' represents the potential of ctDNA to serve as the surrogate material of tumor tissue that is only obtainable by surgical methods.

Rhabdomyosarcoma (RMS), the most frequent soft tissue tumor in childhood,[6] is a malignant small round-cell tumor considered to arise from primitive mesenchymal progenitors with a limited capacity of myogenic differentiation.[7] Pathologically, RMS is broadly categorized into the embryonal, alveolar, and pleomorphic, and spindle cell/sclerosing subtypes. Up to 90% of alveolar RMS cases present with a translocation of t(2;13)(q35;q14), or less frequently, t(1;13)(p36;q15).[8,9] Both involve the DNA-binding domain of *PAX*, a member of the paired box family of transcription

factors, and *FOXO1*/*FKHR*, a member of the forkhead/HNF-3 transcription factor family. The t(2;13) translocation results in the fusion of the *PAX3* gene with *FOXO1*, while the t(1;13) translocation fuses *PAX7* with *FOXO1*.

The outcome of alveolar RMS with the *PAX3-FOXO1* fusion is still unsatisfactory.[10,11] Because tumor volume is one of the determinants of treatment response and outcome,[12] early detection at diagnosis, as well as during the course of the therapy, is a possible strategy to improve the treatment outcome. RMS, as well as other soft tissue tumors, frequently arise in deep parts of the body, and sometimes, in inoperable locations. In such situations, radiological imaging is the only available method for disease burden estimation and prediction/detection of disease recurrence, as there are no useful biological markers present in the blood. Although several imaging analyses, such as ^{18}F-fluoro-2-deoxy-D-glucose positron emission tomography (FDG-PET) scanning, are useful for the evaluation of tumor location and burden, these imaging methods are not sensitive enough to detect the early phase of the disease at the diagnosis and relapse stages. In addition, frequent image analysis is usually difficult to perform because of cost and affordability issues. More convenient methods, which could detect the tumor at the early phases, may be necessary and useful for the management of soft tissue tumors such as RMS in childhood.

A tumor-specific fusion gene could be the most reliable marker for this purpose, as it usually occurs at the initial stages and becomes a genetic abnormality that is essential for tumor survival. We used liquid biopsies, with the tumor-specific *PAX3-FOXO1* fusion as the marker, for examining a case of alveolar RMS with bone marrow invasion.

2 MATERIALS AND METHODS

2.1 Patient

A 15-year-old male patient with lumbago and hematuria was diagnosed with an intrapelvic tumor at the prostate, and swelling of the surrounding lymph nodes was observed by abdominal CT. FDG-PET scanning showed FDG uptake in the tumor mass in the pelvis and in the bone marrow (Figure S1A). Bone marrow aspiration from the iliac bone confirmed the presence of non-hematopoietic tumor cells (Figure S1B) that were positive for CD56 but negative for CD45. RMS was suspected mainly because the tumor originated in the prostate; molecular analysis was then performed. The *PAX3-FOXO1* fusion was identified, and a diagnosis of alveolar RMS (stage IV) was finally made (Figure S1C). After the diagnosis, combination chemotherapies, followed by autologous peripheral blood stem cell transplantation (auto-PBSCT) in remission, and ionizing radiation therapy (RT, 50 Gy in total) at the primary site of the tumor was performed. FDG-PET scanning prior to the auto-PBSCT showed no active uptake of FDG, indicating a state of complete remission. However, FDG-PET scanning at two months after the auto-PBSCT showed an active uptake of FDG at the right cervical lymph nodes and right femur, indicating the relapse of the disease. Although several chemotherapies were provided to the patient after relapse, the tumors became uncontrollable and his general condition gradually worsened. Finally, the patient was transferred to palliative care about six months after relapse; he died shortly thereafter.

Results of the karyotypic analysis of bone marrow samples performed at several time points are shown in Table S1, and details of the therapies that the patient underwent are briefly summarized in Table S2.

Peripheral blood and bone marrow cells were collected from the patient, and used for the study. In accordance with the Declaration of Helsinki, written informed consent was obtained from the patient and the parents, and all research was approved by the institutional review board at Ehime University.

2.2 Detection of the *PAX3-FOXO1* genomic fusion in blood plasma

The genomic breakpoints of the *PAX3* and *FOXO1* genes in tumor cells were identified by inverse polymerase chain reaction (PCR) on bone marrow cell samples at diagnosis, the details of which are described in the supporting information section. Plasma samples were collected from the peripheral blood of the patient and cfDNA was isolated using the MagMAX Cell-Free DNA Isolation Kit (Thermo Fisher Scientific, Waltham, MA USA), according to the manufacturer's instructions. A total of 1.2 mL of plasma was used for cfDNA extraction on most of the occasions and finally eluted using 20 μL of elution solution included in the isolation kit. The PCR amplification of the *PAX3-FOXO1* fusion gene was performed with a pair of forward primers located in intron 7 of the *PAX3* gene and a reverse primer located in intron 1 of the *FOXO1* gene, using the SapphireAmp Fast PCR Master Mix (Takara, Otsu, Japan), according to the manufacturer's instructions. The second round of PCR was performed with a 1-μL aliquot from the first amplification product using internally located pairs of nested primers. Strict precautions were followed to prevent the cross-contamination of samples, and multiple negative controls were always included in each PCR amplification step. The positive control samples obtained at the diagnosis stage and positively amplified PCR products were handled only during the sensitivity assays of the PCR and qPCR analyses. These positive DNA samples were never handled during the actual analyses,

for which the samples obtained during the follow-up of the patient were used. Each PCR analysis was repeated at least thrice to confirm that the results are consistent.

The PCR products were electrophoresed on an agarose gel, and the positive bands were eluted from the gel, purified with a QIAquick Gel Extraction kit (Qiagen, Hilden, Germany), and directly sequenced to confirm the amplification of the fusion gene. Details of the primers are listed in Table S3.

2.3 Quantification of the *PAX3-FOXO1* fusion gene in blood plasma cfDNA

The quantification of the *PAX3-FOXO1* fusion gene in plasma cfDNA was assessed by quantitative PCR (qPCR) using the PowerUp SYBR Green Master Mix (Applied Biosystems, Foster City, CA, USA), according to the manufacturer's instructions. *PGK2* was used as an endogenous control and reference. All measurements were carried out in duplicate, and the difference in the duplicate threshold cycles was less than one cycle in all the samples analyzed. All experiments were repeated at least thrice. The primers used for qPCR are listed in Table S3.

2.4 Sensitivity of conventional and quantitative PCRs for detecting the *PAX3-FOXO1* fusion

The purified PCR product spanning the *PAX3-FOXO1* fusion point was serially diluted and subjected to amplification by nested PCR and qPCR to assess the sensitivity of the PCR. A constant amount (10 ng) of genomic DNA without the *PAX3-FOXO1* fusion was mixed with the serially diluted PCR product.

3 RESULTS

3.1 Plasma cfDNA is useful for the detection of the *PAX3-FOXO1* fusion gene

Reverse transcriptase-PCR analysis of tumor cells in the bone marrow of the patient showed the amplification of the *PAX3-FOXO1* fusion gene (Figure S1C). Direct sequencing analysis confirmed an in-frame fusion of exon 7 of *PAX3* to exon 2 of *FOXO1* (Figure 1A). The genomic junction of the *PAX3* and *FOXO1* genes was identified by inverse PCR targeted on intron 7 of the *PAX3* gene (Figure S2). As shown in Figure 1B, a short inverted genomic sequence derived from intron 7 of the *PAX3* gene was inserted between the genomic *PAX3* and *FOXO1* sequences. A pair of primers was designed to detect the *PAX3-FOXO1* genomic fusion by PCR as shown in Figure 2A. Tumor cells in the bone marrow sample obtained at relapse, which were separated as the $CD45^-$ $CD56^+$ population (Figure S3A), showed positive amplification of the *PAX3-FOXO1* fusion gene by genomic PCR performed using these primers (Figure S3B). Bone marrow mononuclear cells at diagnosis as well as at relapse also showed positive amplification of the *PAX3-FOXO1* fusion, as expected (Figure 2B).

Plasma was separated from the peripheral blood of the patient at relapse, and cfDNA extracted from the plasma was examined for the detection of the *PAX3-FOXO1* fusion by PCR. The *PAX3-FOXO1* fusion could be detected in the cfDNA at relapse by nested PCR (Figure 2C), and the amount of the *PAX3-FOXO1* fusion in the cfDNA samples was quantifiable by qPCR (Figure 2D).

The sensitivity of the PCR for the *PAX3-FOXO1* genomic fusion was assessed on the serially diluted *PAX3-FOXO1*-containing amplified PCR product (450 bp in length). After calculation, one copy of double-stranded DNA of the PCR product was found to correspond to 5×10^{-7} pg of DNA. In the nested PCR amplification, the primer pairs used for the analysis were able to detect as little as 1×10^{-6} pg of fusion DNA, which roughly

corresponded to two copies of *PAX3-FOXO1*, i.e., two tumor cells (Figure 3A). In the qPCR analysis, the *PAX3-FOXO1* fusion sequence was consistently amplified with as little as 1×10^{-5} pg of fusion DNA, which corresponded to approximately 20 tumor cells with the fusion sequence (Figure 3B). The relative dosage of the *PAX3-FOXO1* fusion gene is comparable within the indicated range of the sample DNA concentrations. Even with 1×10^{-6} pg of DNA, the *PAX3-FOXO1* fusion could be detected by qPCR, although only two out of eight runs yielded detectable results with specific amplification (Figure 3C).

3.2 Early detection of the *PAX3-FOXO1* fusion in cfDNA preceding the relapse stage

The amount of the *PAX3-FOXO1* fusion gene was serially evaluated using cfDNA obtained at different time points during the course of the treatments. The time points at which the cfDNA samples were collected are shown in Figure 4A, along with the results of FDG-PET scanning, which was performed serially, in Figure 4B and 4C.

After the initial chemotherapy following diagnosis, tumor cells in the bone marrow disappeared and became undetectable by reverse transcriptase-PCR analysis using RNA samples extracted from the bone marrow cells (data not shown). Because the obtained bone marrow cells were not sufficient for DNA extraction, quantification of the fusion gene dosage in the DNA samples from the bone marrow was not performed at this point. In addition, plasma cfDNA also turned out to be negative for the *PAX3-FOXO1* fusion, indicating a significant loss of tumor cells in the body (“a” in Figure 5A). However, the *PAX3-FOXO1* fusion became detectable in the nested conventional PCR analysis of plasma cfDNA shortly after the negative result was

obtained (“c” in Figure 5B, upper panel). Although qPCR showed a negative result at this point (“c”), the *PAX3-FOXO1* fusion gene was detectable by qPCR at the point (“d” in Figure 5A) where FDG-PET scanning had not yet shown the presence of the tumor cells; this point was judged as the complete remission stage (CR), as shown in Figure 4B. Auto-PBSCT conducted after the point (d), with the judgement of CR solely by FDG-PET scanning, could not reduce the tumor burden, and eventually, FDG-PET scanning detected the focal relapse in the cervical lymph nodes and femur (“e”, Figure 4B) accompanied by the increase in the *PAX3-FOXO1* gene dosage in the cfDNA (“e” in Figure 5A). After the recognition of focal recurrence, the tumor lesions rapidly expanded in the patient, including their expansion in the bone marrow, as shown in Figure 4C, accompanied by an apparent relapse in the bone marrow and a continuous increase in the *PAX3-FOXO1* gene dosage in the cfDNA (“f” in Figure 5A). According to qPCR analysis, the gene dosage of non-rearranged *PAX3*, which was used as an endogenous control, was estimated to be constantly stable during the treatments (Figure 5A, lower panel).

Because the DNA extracted from erythrocyte-depleted peripheral blood cells, even after the bone marrow infiltration of tumor cells became apparent, never presented positive results for the *PAX3-FOXO1* fusion (Figure 5B, lower panel), the positivity of the *PAX3-FOXO1* fusion is attributed to the ctDNA derived from tumor cells somewhere in the body, rather than from the circulating tumor cells in the blood.

3.3 Plasma cfDNA is a useful marker for the assessment of tumor volume

Upon relapse, several chemotherapy sessions, as well as radiation therapy, were conducted. Gene dosage of the *PAX3-FOXO1* fusion was monitored in cfDNA samples

by qPCR (Figure 5C) and conventional PCR analyses (Figure 5D). The *PAX3-FOXO1* fusion gene dosage fluctuated from positive to barely detectable, reflecting the timing of the chemotherapy administered to the patient. In all situations, the *PAX3-FOXO1* fusion became undetectable by qPCR analysis a few days after the treatment, and became positive again before the succeeding treatment. The gene dosage of non-rearranged *PAX3*, which was estimated by qPCR, was constantly stable during the treatments.

4 DISCUSSION

cfDNA is considered to represent the genetic profile of cells in the body, including tumor(s) existing anywhere in the body. Although RMS and other soft tissue tumors could occur anywhere, tumor-derived circulating DNA, which is called ctDNA, should be present among the cfDNA. The cfDNA can be readily extracted from the blood plasma. Additionally, the sampling of blood plasma is easy, making cfDNA a suitable source for cancer detection. With cfDNA as the sample for genetic analysis, the detection and follow-up of cancer cases can be facilitated by the identification of cancer-related genetic change(s), such as *KRAS* mutations. Although such genetic changes are frequently observed in cancer at the diagnosis and relapse stages, they may not be essential, first hit events in cancer development in most cases. In addition, because of the heterogeneity among tumor cells, these genetic changes may not be present in all tumor cells. This problem becomes crucial in the follow-up of the tumor because the absence of certain mutation(s) originally identified in tumor cells may not necessarily indicate the disappearance of the tumor.[13,14]

Similar to the case for hematological malignancies, tumor-specific fusion gene formation is one of the hallmarks of soft tissue tumors; the formation of most fusion

genes is considered a first hit event that is essential for cancer development.[15,16] In this regard, fusion genes are the most suitable biological markers for cancer detection. Using specific PCR primers, the detection of such fusion sequences is possible by relatively straightforward PCR targeted towards junction sequences, without any need for allele-specific PCR. In addition, targeting tumor-specific fusion sequences is associated with high specificity even in the presence of misleading, age-related clonal hematopoiesis with cancer-related mutation(s), because such fusion sequences are otherwise absent in non-tumor cells. However, till date, only a few studies regarding the usage of tumor-specific fusion genes as the biomarkers of soft tissue tumors in liquid biopsy have been reported,[17-21] including a recent study reporting the detection of *PAX3* fusion in the cfDNA of alveolar RMS samples by next-generation sequencing.[21]

One important pitfall of using the tumor-specific fusion gene as a biomarker is the possibility of the tumor progressing to a fusion-independent state due to the acquisition of other genetic abnormalities after therapeutic interventions are performed for the primary tumor. The actual progression to a *PAX3-FOXO1*-independent state during the recurrence of the tumor has been reported recently in a mouse model.[22] Therefore, fusion-specific assays may become problematic in the later stages of tumor progression in some cases, particularly in settings involving treatment with targeted agents that may enhance clonal selection inside the tumors.

Apart from tumor-specific fusion genes, other tumor-specific genomic rearrangements such as deletions and amplifications have been investigated in several types of cancers by the application of the whole-genome sequencing technology.[23,24] Monitoring these rearrangements together with the fusion gene may provide more reliable results wherever possible.

The genomic junctional sequence of *PAX3-FOXO1* in the patient was determined by inverse PCR technology. The insertion of a short inverted sequence at the junction is not a common way for double-strand break (DSB) repair, which is observed in many types of tumors. There are no consensus recognition sequences for DNA breaks, such as those caused by Topoisomerase-II, around the genomic junction. Although the mechanism of the insertion is unclear, a possible mechanism underlying the gene fusion is a non-homologous end-joining step, as only the insertion and overlap of a few bases were observed at the junction.[25]

A recently developed approach of partial genome sequencing following the hybrid capture of a set of defined sequences may be a useful method to identify tumor-specific genomic junctional sequences.[19,21] An obvious advantage of the hybrid capture approach is its applicability to formalin-fixed tumor materials and cfDNA samples. Considering the present clinical settings, where sufficient amounts of fresh/frozen materials for inverse PCR are unavailable in many occasions, the hybrid capture approach may currently be the most optimal method for the detection of tumor-specific fusion sequences.

We identified the *PAX3-FOXO1* fusion gene in the plasma cfDNA of a patient with alveolar RMS, and used this fusion as a marker for cancer detection during the treatment course. As shown in Figure 2, cfDNA could be an appropriate source for the detection of the *PAX3-FOXO1* fusion. Conventional PCR amplification is useful to confirm the presence of the fusion sequence and corresponding tumor cells, without the need for an allele-specific or mutation-specific amplification system mainly used in earlier studies; however, strict precautions are necessary to avoid any contaminations, which may result in false-positive results. As reported previously,[13,26-29] an assay using

cfDNA has been proven to be useful for the early detection of tumor progression/recurrence. In the nested PCR analysis for the *PAX3-FOXO1* fusion using plasma cfDNA samples, the fusion sequence turned out to be detectable at the 'remission stage', when imaging analyses such as FDG-PET scanning could not detect any recurrence of the tumor (Figures 4 and 5B).

Estimation of the *PAX3-FOXO1* fusion gene dosage by qPCR, corresponding to the dosage of the ctDNA, is quite useful for monitoring the tumor burden in the body. Although the fusion was absent in the qPCR analysis of the cfDNA when conventional nested PCR first detected it, the qPCR results subsequently turned out to be positive approximately 50 days after the positive result for the conventional PCR analysis was obtained, and more than 4 months earlier than the recognition of the relapse by FDG-PET scanning (Figure 4 and 5A). This delay in the detection of the fusion gene is possibly attributed to a difference in the sensitivity between the nested PCR and qPCR analyses, as shown in Figure 3. More frequent sampling and analysis of cfDNA could possibly detect the fusion sequence by qPCR earlier than the time point (d), because the difference in sensitivity between the two methods is only tenfold. In addition, analyses with large amounts of cfDNA could increase the sensitivity especially when the amount of the targeting sequences is low. In this regard, as reported previously, absolute quantification using the droplet digital PCR (ddPCR) technology could also be a suitable method for detecting pediatric soft tissue tumors whenever possible.[17-19]

The estimated fusion gene dosage increased until the commencement of treatment after relapse, possibly indicating the increasing tumor burden of the overt relapse. In summary, the fusion gene dosage estimated by qPCR efficiently reflects the number of tumor cells at the remission stage and during the course of the treatment (Figure 2D).

Shortly after the chemotherapy, the levels of the fusion gene consistently declined and increased again before the next treatment course. A relatively stable level of the endogenous, non-rearranged *PAX3* gene, which was estimated by qPCR, indicated the reliability of the method; on the other hand, fluctuating levels of the fusion gene may reflect the state of the tumor in the body. In addition, a rapid decline of the *PAX3-FOXO1* fusion after chemotherapy and immediate increase afterwards possibly reflects the temporary reduction of tumor volume by chemotherapy. These observations indicate that the administered chemotherapies were effective but not adequate. Due to the very short half-life of cfDNA in plasma,[1] monitoring ctDNA may be useful for the early detection of tumors anywhere in the body, and for the evaluation of the response to therapy.[30]

Because tumor-specific fusion genes are early genetic hits essential for tumor sustenance and are easily amplifiable by PCR, they could serve as reliable and convenient targets for monitoring the disease. Once the tumor-specific fusion gene is identified in tumor samples at the diagnosis or relapse stages, it could be available for use in the assays using cfDNA samples.

Recently, the detection of tumor-specific *EWSR1* fusion genes in the liquid biopsy of Ewing sarcoma samples using two different methodologies has been reported.[17,20] Hayashi et al. used patient-specific genomic fusion sequences of ctDNA as tumor biomarkers in circulating blood,[17] while Allegretti et al. used circulating tumor RNA (ctRNA) with *EWSR1* fusion transcripts as a tumor biomarker.[20] Both methods proved the tumor-specific fusion gene to be useful in monitoring the tumor volume and for the follow-up of patients with Ewing sarcoma, as described in this report regarding RMS. A drawback of the method using cfDNA and genomic fusion sequences against that using

ctRNA is the necessity of fresh tumor samples to identify the breakpoint sequences, since formalin-fixed tumor samples are sometimes unsuitable for inverse PCR or long-distance PCR owing to DNA fragmentation. Although this difficulty may be overcome by the application of whole-genome sequencing of cfDNA samples for the identification of unknown fusion sequences,[23] considering that pathological diagnosis is mandatory for the accurate diagnosis of any soft tissue tumor, this problem may be solved if even a small portion of the diagnostic sample can be used for determining the fusion breakpoint sequence before the sample is fixed in formalin. Further studies are necessary to determine the preferable approach for actual clinical use.

Herein, we report the clinical benefits of detecting patient-specific fusion gene sequences by liquid biopsy as a biomarker of soft tissue tumors. This is the first report of a detailed follow-up of a case of RMS using cfDNA samples. Since the isolation of genomic breakpoints by inverse PCR or long-distance PCR is not a cumbersome procedure, for fusion gene-positive RMS, as well as other soft tissue tumors, tumor-specific fusion sequences should be used for monitoring the tumor burden in the body for diagnostic and therapeutic purposes.

Acknowledgement

The authors would like to thank Ms. Chihiro Tanaka, Ms. Tokiko Mizushiro, Yuko Kajita, and Ms. Mio Ishimaru for their technical assistance. We would like to thank Editage (www.editage.jp) for their help with English language editing. This work was supported by the Japan Leukemia Research Fund.

References

1. Yao W, Mei C, Nan X, Hui L. Evaluation and comparison of in vitro degradation kinetics of DNA in serum, urine and saliva: A qualitative study. *Gene.* 2016;590(1):142-148.
2. Cheng F, Su L, Qian C. Circulating tumor DNA: A promising biomarker in the liquid biopsy of cancer. *Oncotarget.* 2016;7(30):48832-48841.
3. Volik S, Alcaide M, Morin RD, Collins C. Cell-free DNA (cfdna): Clinical significance and utility in cancer shaped by emerging technologies. *Mol Cancer Res.* 2016;14(10):898-908.
4. Wan JCM, Massie C, Garcia-Corbacho J, et al. Liquid biopsies come of age: Towards implementation of circulating tumour DNA. *Nat Rev Cancer.* 2017;17(4):223-238.
5. Jahr S, Hentze H, Englisch S, et al. DNA fragments in the blood plasma of cancer patients: quantitations and evidence for their origin from apoptotic and necrotic cells. *Cancer Res.* 2001;61(4):1659-1665.
6. Ducimetière F, Lurkin A, Ranchère-Vince D, et al. Incidence of sarcoma histotypes and molecular subtypes in a prospective epidemiological study with central pathology review and molecular testing. *PLoS One.* 2011;6(8):e20294.
7. Merlino G, Helman LJ. Rhabdomyosarcoma--working out the pathways. *Oncogene.* 1999;18(38):5340-5348.
8. Barr FG, Galili N, Holick J, Biegel JA, Rovera G, Emanuel BS. Rearrangement of the PAX3 paired box gene in the paediatric solid tumour alveolar rhabdomyosarcoma. *Nat Genet.* 1993;3:113.
9. Davis RJ, D'Cruz CM, Lovell MA, Biegel JA, Barr FG. Fusion of PAX7 to

FKHR by the variant t(1;13)(p36;q14) translocation in alveolar rhabdomyosarcoma. *Cancer Res.* 1994;54(11):2869-2872.

10. Missiaglia E, Williamson D, Chisholm J, et al. PAX3/FOXO1 fusion gene status is the key prognostic molecular marker in rhabdomyosarcoma and significantly improves current risk stratification. *J Clin Oncol.* 2012;30(14):1670-1677.
11. Skapek SX, Anderson J, Barr FG, et al. PAX-FOXO1 fusion status drives unfavorable outcome for children with rhabdomyosarcoma: A children's oncology group report. *Pediatr Blood Cancer.* 2013;60(9):1411-1417.
12. Eilber FC, Brennan MF, Riedel E, Alektiar KM, Antonescu CR, Singer S. Prognostic factors for survival in patients with locally recurrent extremity soft tissue sarcomas. *Ann Surg Oncol.* 2005;12(3):228-236.
13. Fernandez-Cuesta L, Perdomo S, Avogbe PH, et al. Identification of circulating tumor DNA for the early detection of small-cell lung cancer. *EBioMedicine.* 2016;10:117-123.
14. Hu Y, Ulrich BC, Supplee J, et al. False-positive plasma genotyping due to clonal hematopoiesis. *Clin Cancer Res.* 2018.
15. Oda Y, Yamamoto H, Kohashi K, et al. Soft tissue sarcomas: From a morphological to a molecular biological approach. *Pathol Int.* 2017;67(9):435-446.
16. Mertens F, Antonescu CR, Mitelman F. Gene fusions in soft tissue tumors: Recurrent and overlapping pathogenetic themes. *Genes Chromosomes Cancer.* 2016;55(4):291-310.
17. Hayashi M, Chu D, Meyer CF, et al. Highly personalized detection of minimal Ewing sarcoma disease burden from plasma tumor DNA. *Cancer.*

2016;122(19):3015-3023.

18. Krumbholz M, Hellberg J, Steif B, et al. Genomic EWSR1 fusion sequence as highly sensitive and dynamic plasma tumor marker in Ewing sarcoma. *Clin Cancer Res.* 2016;22(17):4356-4365.

19. Shukla NN, Patel JA, Magnan H, et al. Plasma DNA-based molecular diagnosis, prognostication, and monitoring of patients with EWSR1 fusion-positive sarcomas. *JCO Precis Oncol.* 2017;2017.

20. Allegretti M, Casini B, Mandoj C, et al. Precision diagnostics of Ewing's sarcoma by liquid biopsy: circulating EWS-FLI1 fusion transcripts. *Ther Adv Med Oncol.* 2018;10:1758835918774337.

21. Klega K, Imamovic-Tuco A, Ha G, et al. Detection of somatic structural variants enables quantification and characterization of circulating tumor DNA in children with solid tumors. *JCO Precis Oncol.* 2018;2018(2):1-13.

22. Pandey PR, Chatterjee B, Olanich ME, et al. PAX3-FOXO1 is essential for tumour initiation and maintenance but not recurrence in a human myoblast model of rhabdomyosarcoma. *J Pathol.* 2017;241(5):626-637.

23. Leary RJ, Sausen M, Kinde I, et al. Detection of chromosomal alterations in the circulation of cancer patients with whole-genome sequencing. *Sci Transl Med.* 2012;4(162):162ra154.

24. Heitzer E, Ulz P, Belic J, et al. Tumor-associated copy number changes in the circulation of patients with prostate cancer identified through whole-genome sequencing. 2013;5(4):30.

25. Seki Y, Mizukami T, Kohno T. Molecular process producing oncogene fusion in lung cancer cells by illegitimate repair of DNA double-strand breaks.

Biomolecules. 2015;5(4):2464-2476.

26. Heitzer E, Perakis S, Geigl JB, Speicher MR. The potential of liquid biopsies for the early detection of cancer. *Precision Oncol.* 2017;1(1):36.

27. Chaudhuri AA, Chabon JJ, Lovejoy AF, et al. Early detection of molecular residual disease in localized lung cancer by circulating tumor DNA profiling. *Cancer Discov.* 2017;7(12):1394-1403.

28. Abbosh C, Birkbak NJ, Wilson GA, et al. Phylogenetic ctDNA analysis depicts early-stage lung cancer evolution. *Nature.* 2017;545(7655):446-451.

29. Cohen JD, Li L, Wang Y, et al. Detection and localization of surgically resectable cancers with a multi-analyte blood test. *Science.* 2018;359(6378):926-930.

30. Diehl F, Schmidt K, Choti MA, et al. Circulating mutant DNA to assess tumor dynamics. *Nat Med.* 2008;14(9):985-990.

Figure legends

Figure 1

Isolation of the genomic breakpoints of the *PAX3-FOXO1* fusion gene. (A) Identification of an in-frame *PAX3-FOXO1* fusion by reverse transcriptase-polymerase chain reaction. Direct sequencing analysis of the amplified product (Figure S1C) showed a fusion of exon 7 of *PAX3* to exon 2 of *FOXO1*. The red arrow indicates the junction point of the fusion transcript. (B) A genomic breakpoint identified by direct sequencing analysis of the purified rearranged product obtained by inverse PCR (Figure S2). The horizontal arrows in green and red indicate the sequences derived from the *FOXO1* and *PAX3* genes, respectively. The directions of the arrow indicate the 5′ to 3′ position of the genes. The short sequence from *PAX3* intron 7 adjacent to the breakpoint is inverted and inserted between the junction of the *PAX3* and *FOXO1* sequences. Four bases (TCAC) of unknown origin are also inserted at the genomic junction of *PAX3* and *FOXO1*.

Figure 2

Detection and identification of the *PAX3-FOXO1* fusion gene in the plasma cfDNA of the patient. (A) Genomic breakpoints of the *PAX3-FOXO1* fusion gene, and the primers designed for the detection of the fusion gene in the plasma cfDNA sample. A short inverted sequence from *PAX3* intron 7 is inserted between the junction of the *PAX3* and *FOXO1* sequences. The horizontal arrows in grey and black indicate sequences derived from the *PAX3* and *FOXO1* genes, respectively. The directions of the arrow indicate the 5′ to 3′ position of the genes. A pair of forward and reverse primers for the detection of the genomic fusion sequence is indicated by a pair of black dotted arrows. Although

several pairs of primers for nested PCR were designed, the locations of the primers designed at the most internal position are shown. (B) Detection of the *PAX3-FOXO1* fusion gene with these primers in bone marrow samples collected at the diagnosis and relapse stages. DNA was extracted from bone marrow mononuclear cells without the flow-sorting of the tumor cells. The fusion gene is amplified only in the patient samples. (C) Detection of the *PAX3-FOXO1* fusion gene in plasma cfDNA. The designed primer pairs for the detection of the fusion gene are valid without yielding any non-specific amplification in control samples. (D) Quantification of the *PAX3-FOXO1* fusion gene in cfDNA by quantitative PCR. The fusion gene is absent in cfDNA obtained at the remission stage, as well as in control samples. *PGK2* was used as an internal reference. CR: complete remission.

Figure 3

Validity and sensitivity of conventional and quantitative PCRs for detecting the *PAX3-FOXO1* fusion gene. (A) Sensitivity of conventional nested PCR with the primer pairs used in the experiments for detecting the fusion gene is shown in Figure 2B and 2C. The serially diluted PCR product (1×10^{-2} to 1×10^{-8} pg) spanning the *PAX3-FOXO1* genomic fusion point was used as the template DNA. A constant amount (10 ng) of genomic DNA without the *PAX3-FOXO1* fusion was mixed with the serially diluted PCR product. After calculation, approximately 1×10^{-6} pg of the PCR product was found to correspond to two copies of *PAX3-FOXO1*, i.e. two tumor cells. (B) Standard curve of the threshold cycle for the amplification of *PAX3-FOXO1* by quantitative PCR (qPCR) is shown. A PCR product serially diluted to 1×10^{-5} pg was used as the template DNA for PCR. The relative dosage of the *PAX3-FOXO1* fusion gene is comparable

within the indicated range of DNA concentrations. (C) Amplification plot of qPCR analysis for detecting the *PAX3-FOXO1* fusion using the PCR product DNA diluted to 1×10^{-6} pg. Representative results of eight duplicate samples are shown. In two out of eight samples (numbers 5 and 7), the fusion gene was detectable by qPCR. The eight different colored boxes with numerical digits correspond to each sample.

Figure 4

Chronological results of the FDG-PET analyses. (A) Time course of the collection of plasma samples from the patient ("a" to "o"), as well as the timings of FDG-PET analysis along with the number of days after diagnosis. The day on which the initial PET analysis was carried out was considered the point of diagnosis and set as day 0. The timings of FDG-PET scanning are indicated by rectangles with upward arrows under the line. The timings of sample collection are indicated by alphabets in lower case ("a" to "o") with downward arrows. The timing of relapse, which was diagnosed by positive FDG-PET scanning results, is also marked with an arrowhead. (B) Results of FDG-PET scanning until relapse. The sites of focal relapse detected in PET-3 are circled. (C) Results of FDG-PET scanning after relapse.

Figure 5

Chronological analysis of the *PAX3-FOXO1* fusion gene in the plasma cfDNA of the patient. Time points of the collection of plasma samples ("a" to "o") are shown in Figure 4A. (A) The changes in the *PAX3-FOXO1* fusion gene dosage in the cfDNA samples estimated by quantitative PCR; the bone marrow samples collected from the diagnosis stage until the relapse stage are shown in the upper panel. *PGK2* was used as

an internal reference. The changes in the *PAX3* gene during the course of the treatments are shown in the lower panel. The arrowheads indicate the time points of diagnosis and relapse. The downward arrows at the top of the graph indicate the time points of chemotherapies. (B) The results of the conventional PCR for detecting the *PAX3-FOXO1* fusion gene in plasma cfDNA (upper panel) and corresponding peripheral blood cells (lower panel). Only the results of the second round of PCR are shown. Peripheral blood DNA was not obtained at time points “b” and “c”. Erythrocytes were removed by hypotonic lysis before the DNA was extracted. (C) The changes in the estimated *PAX3-FOXO1* fusion gene dosage in cfDNA after relapse. The downward arrows at the top of the graph indicate the time points of chemotherapies and the arrowhead indicates the time point of radiation therapy (RT). *PGK2* was used as an internal reference. (D) Results of the conventional PCR at the time point “i” and later. Only the results of the second round of PCR are shown.

Figure 1

A

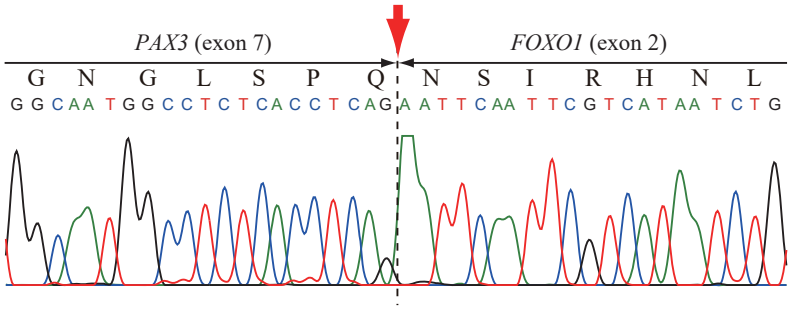
PAX3 (exon 7)
FOXO1 (exon 2)
G N G L S P Q N S I R H N L
G G C A A T G G C C T C T C A C C T C A G A A T T C A A T T C G T C A T A A T C T G

B

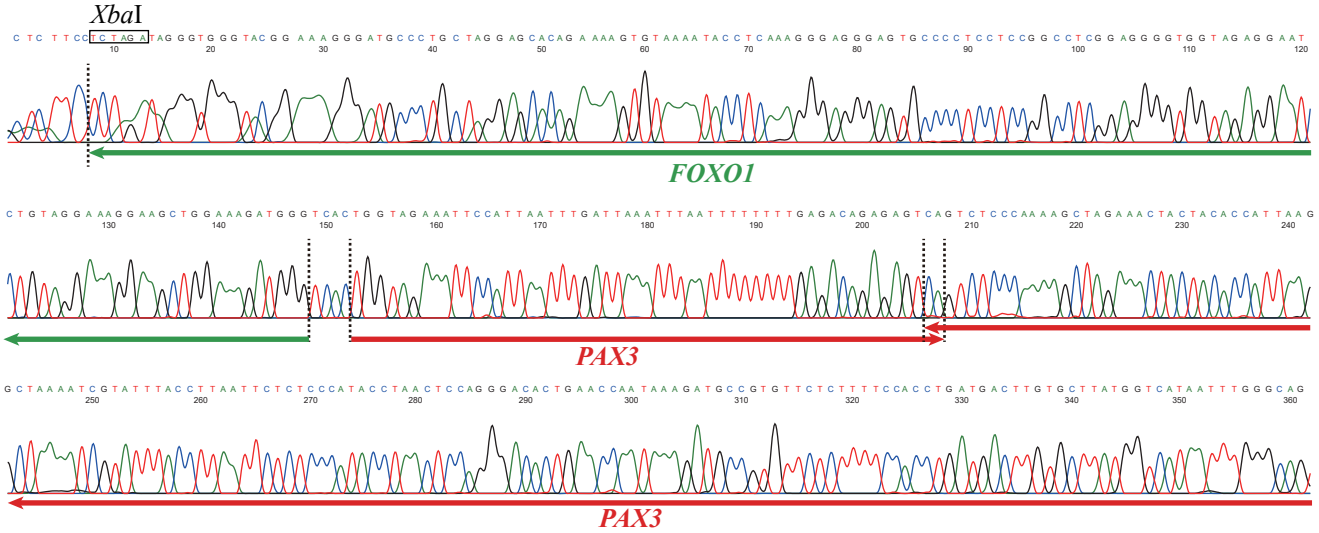
XbaI
FOXO1
PAX3
PAX3

Figure 2

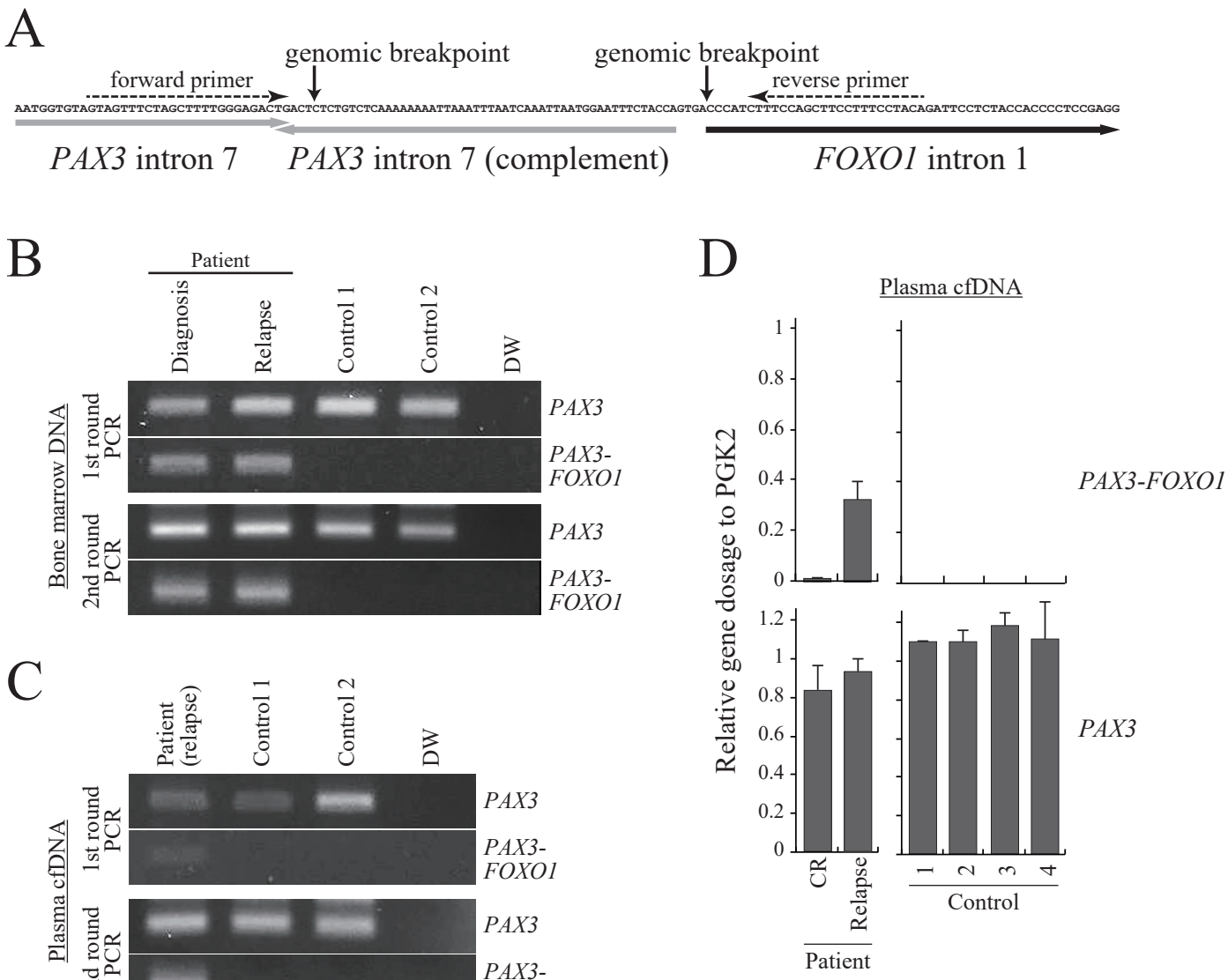
A
genomic breakpoint
genomic breakpoint
forward primer
reverse primer
AATGGTGTAGTAGTTTCTAGCTTTTGGGAGACTGACTCTCTGTCTCAAAAAAAATTAAATTTAATCAAATTAATGGAATTTCTACCAGTGACCCATCTTTCCAGCTTCCTTTCCTACAGATTCCTCTACCACCCCTCCGAGG
PAX3 intron 7
PAX3 intron 7 (complement)
FOXO1 intron 1
B
Patient
Diagnosis
Relapse
Control 1
Control 2
DW
Bone marrow DNA
1st round PCR
2nd round PCR
PAX3
PAX3-FOXO1
C
Patient (relapse)
Control 1
Control 2
DW
Plasma cfDNA
D
Plasma cfDNA
Relative gene dosage to PGK2
PAX3-FOXO1
PAX3
CR
Relapse
Patient
Control

Figure 3

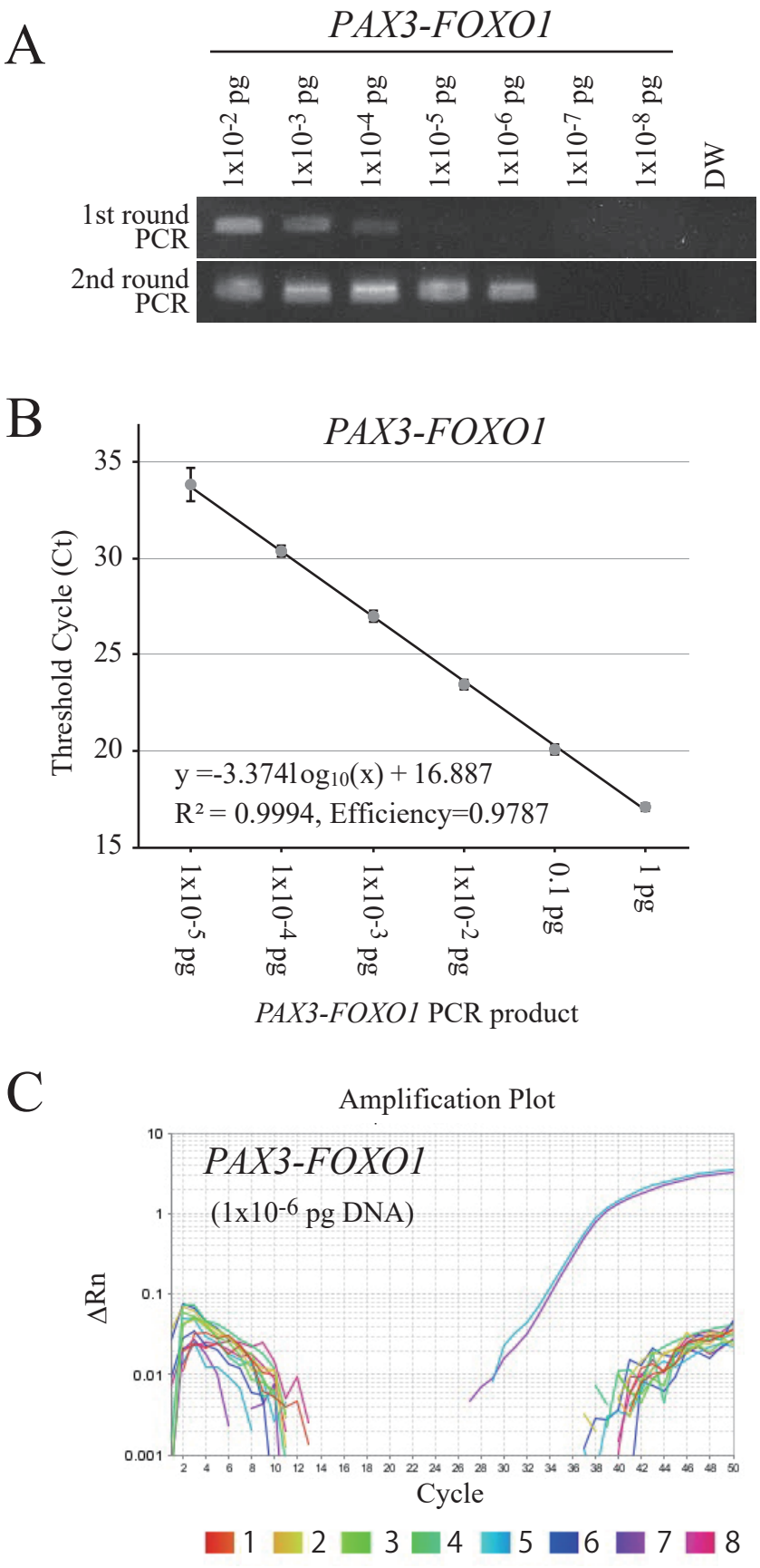
A
PAX3-FOXO1
1x10-2 pg
1x10-3 pg
1x10-4 pg
1x10-5 pg
1x10-6 pg
1x10-7 pg
1x10-8 pg
DW
1st round PCR
2nd round PCR
B
PAX3-FOXO1
Threshold Cycle (Ct)
35
30
25
20
15
y =-3.374log10(x) + 16.887
R2 = 0.9994, Efficiency=0.9787
1x10-5 pg
1x10-4 pg
1x10-3 pg
1x10-2 pg
0.1 pg
1 pg
PAX3-FOXO1 PCR product
C
Amplification Plot
PAX3-FOXO1
(1x10-6 pg DNA)
ΔRn
10
1
0.1
0.01
0.001
2 4 6 8 10 12 14 16 18 20 22 24 26 28 30 32 34 36 38 40 42 44 46 48 50
Cycle
1 2 3 4 5 6 7 8

Figure 4

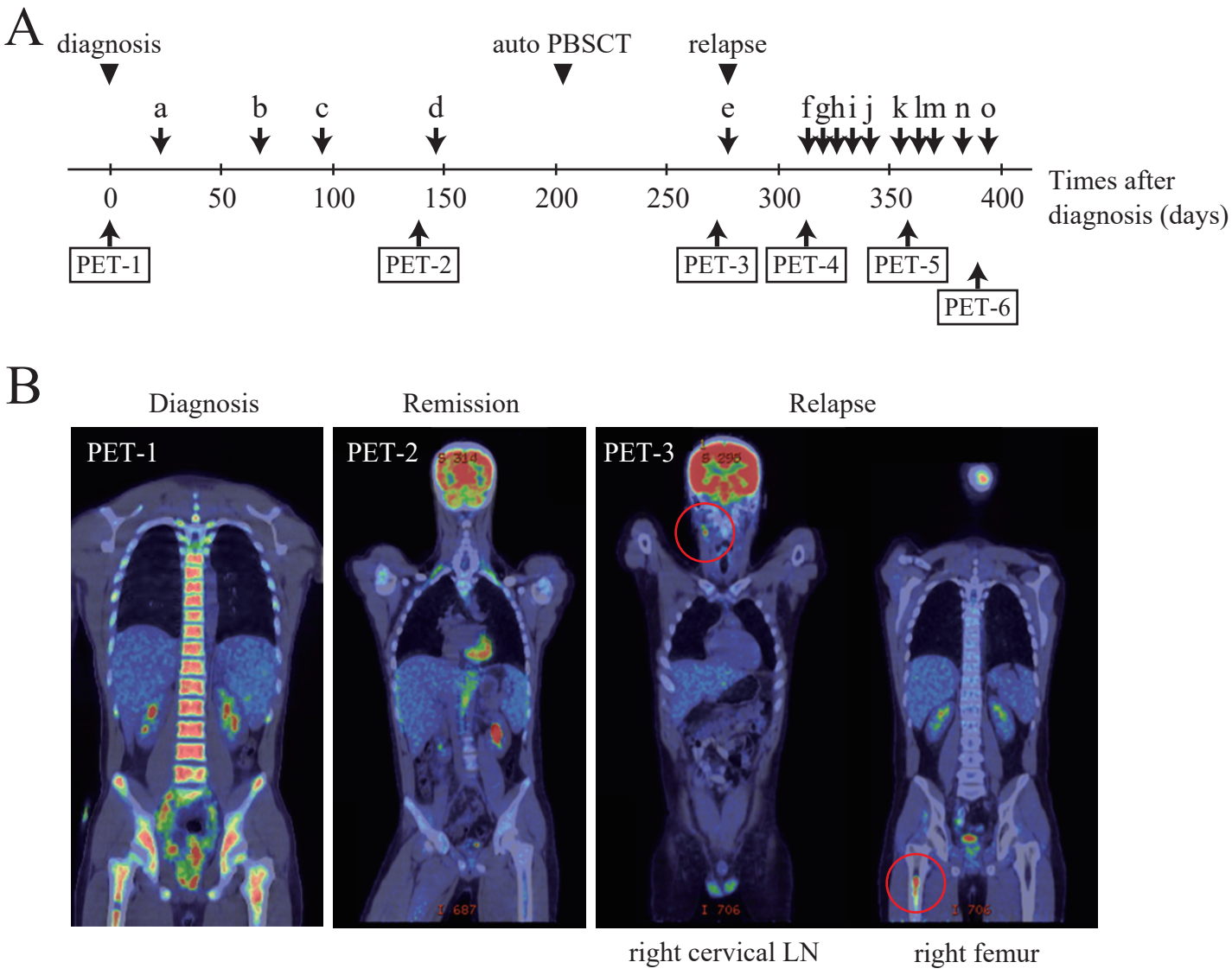
A
diagnosis
auto PBSCT
relapse
a
b
c
d
e
f g h i j
k l m n o
0
50
100
150
200
250
300
350
400
Times after diagnosis (days)
PET-1
PET-2
PET-3
PET-4
PET-5
PET-6
B
Diagnosis
Remission
Relapse
PET-1
PET-2
PET-3
right cervical LN
right femur
C
PET-4
PET-5
PET-6

Figure 5

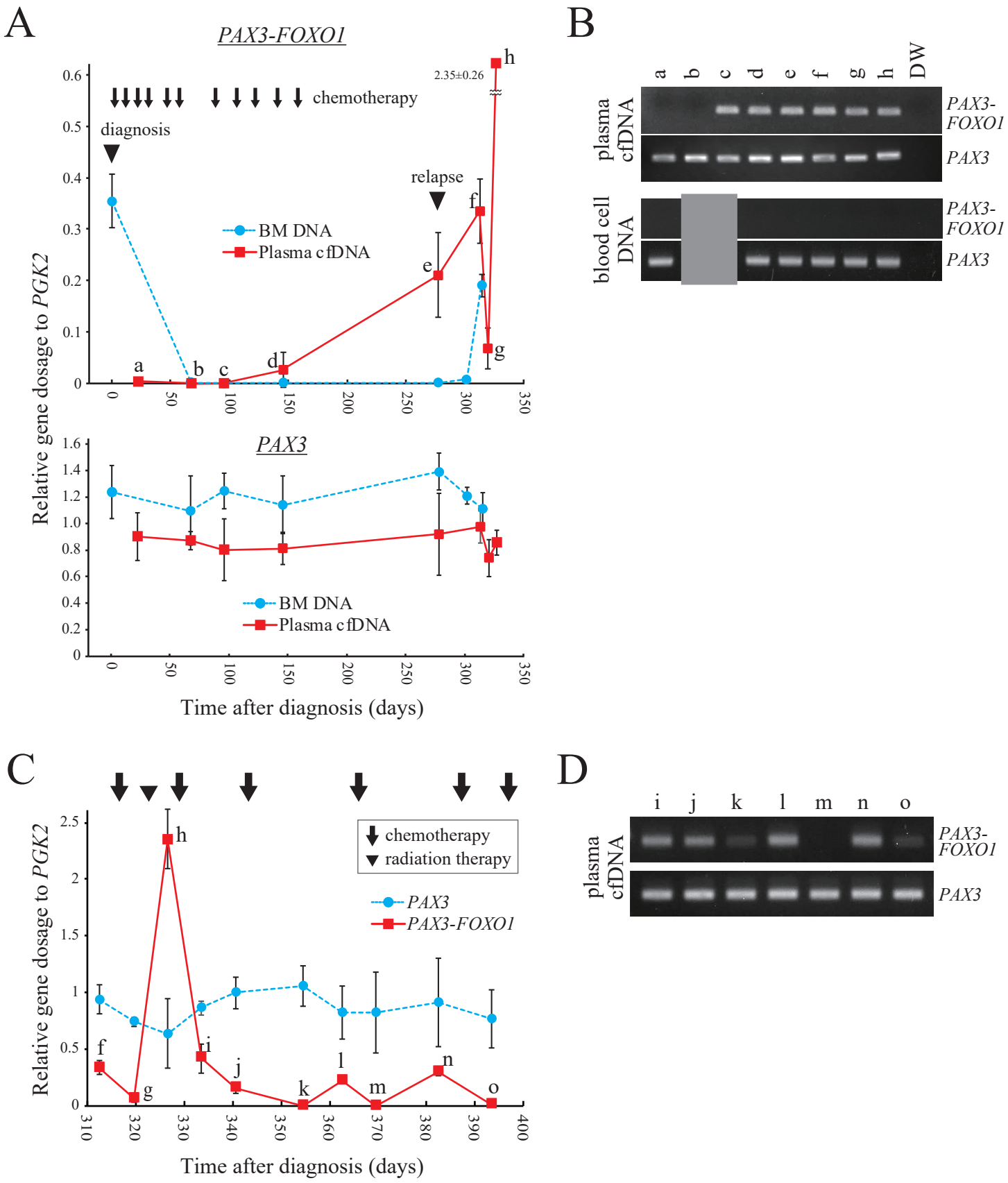
A
PAX3-FOXO1
chemotherapy
diagnosis
relapse
2.35±0.26
BM DNA
Plasma cfDNA
Relative gene dosage to PGK2
PAX3
Time after diagnosis (days)
B
a b c d e f g h DW
plasma cfDNA
blood cell DNA
PAX3-FOXO1
PAX3
C
chemotherapy
radiation therapy
PAX3
PAX3-FOXO1
Relative gene dosage to PGK2
Time after diagnosis (days)
D
i j k l m n o
plasma cfDNA
PAX3-FOXO1
PAX3

Supporting Information

Materials and Methods

Detection of *PAX3-FOXO1* Fusion Transcript by Reverse Transcriptase- Polymerase Chain Reaction (RT-PCR)

Total RNA was extracted from the bone marrow of the patient at diagnosis using an RNeasy Mini kit (Qiagen, Hilden, Germany). The total RNA was reverse-transcribed with a PrimeScript RT-PCR kit (Takara, Otsu, Japan), using a random hexamer according to the manufacturer's instructions. One tenth of the synthesized cDNA was directed to RT-PCR analysis for the detection of the fusion transcript.

In the first round of PCR, reverse primers for fusion partners of *PAX3* as well as *PAX7* were mixed in a single tube together with the forward primer for *PAX3* or *PAX7*. The second round of PCR was performed with the product of first round PCR, which showed a positive product for fusion gene as the PCR template. In the second round of PCR, specific reverse primer for each gene was used in a separate tube with nested forward primer for *PAX3* or *PAX7*. The obtained positive PCR product was cut out from the gel and DNA was purified using QIAquick Gel Extraction kit (Qiagen) and sequenced directly using BigDye Terminator v3.1 Cycle Sequencing kit (Applied Biosystems, Foster City, CA, USA). All sequencing was performed on ABI310 Genetic Analyzer (Applied Biosystems). The primers used are listed in Table S2.

Inverse polymerase chain reaction (PCR)

Inverse PCR was carried out to identify the genomic breakpoint of the *PAX3* and *FOXO1* genes in tumor cells. Genomic DNA was extracted from the bone marrow containing

tumor cells using the standard procedure, and 100 ng of genomic DNA was digested with *EcoR*I and *Xba*I (New England Biolabs, Ipswich, MA, USA). After inactivation of the enzymes and ethanol precipitation, the digested DNA was ligated with T4 DNA ligase (New England Biolabs) at 16 °C overnight. The DNA was precipitated with ethanol and resuspended in 10 μL of sterile water, and used as the template for inverse PCR amplification. The PCR amplification was performed with six pairs of forward and reverse primers, located on intron 7 of the *PAX3* gene near the *EcoR*I and *Xba*I restriction site, using PrimeSTAR GXL DNA polymerase (Takara) according to the manufacturer's instructions. The PCR amplification condition was as follows: 95 °C for 2 min, followed by 35 cycles of 98 °C for 10 s, and 68 °C for 15 min. The second-round of PCR was performed with 1 μL aliquot from the first amplification product, using internally located nested primers. The PCR products were electrophoresed on an agarose gel, and positive bands were eluted from the gel, purified with a QIAquick Gel Extraction kit (Qiagen), and directly sequenced on the ABI310 Genetic Analyzer (Applied Biosystems). Details of the primers are described in Table S2.

Flow cytometry and cell sorting

After erythrocyte lysis with RBC Lysis Buffer (BioLegend, San Diego, CA, USA), the bone marrow cells were stained with a monoclonal antibody according to the manufacturer's instructions and analyzed using Gallios flow cytometer (Beckman Coulter, Brea, CA, USA) and FlowJo software (TreeStar, Ashland, OR, USA). Cell sorting was performed with a FACSAria cell sorter (BD Biosciences, San Jose, CA, USA). The following antibodies were used for the analysis: anti-CD235a phycoerythrin (PE; Biolegend), anti-CD56 Alexa Fluor 647 (Biolegend), anti-CD45 Krome Orange

(Beckman Coulter, Indianapolis, IN). For exclusion of dead cells, 7-Amino-acinomycin D (7-AAD; BioLegend) was used.

Supplementary Table S1

Karyotype of the patient at the different points

Diagnosis
47,XY,add(2)(q21),add(12)(q24.1),del(13)(q?),add(16)(p11.2),+mar1[5]/ 48,idem,+mar1[9]/49,idem,+mar1x2[3]/46,XY[1]
After first cycle of chemotherapy
46,XY[20]
After four cycles of chemotherapy
46,XY[20]
Relapse after auto-PBSCT
89,XXY,-Y,add(2)(q21)X2,-3,-4,add(6)(p21),del(7)(q?),-10, add(12)(q24.1)X2,del(13)(q?)X2,-15,add(16)(p11.2)X2,+2mar[1]/ 46,XY[12]
After five cycles of chemotherapy since relapse
88,XXY,-Y,add(2)(q21)X2,-3,-4,add(6)(p21),+del(7)(q?),-10, add(12)(q24.1)X2,del(13)(q?)X2,-15,add(16)(p11.2)X2,-19,+2mar[1]/ 46,XY[17]

auto-PBSCT, autologous peripheral blood stem cell transplantation

Supplementary Table S2

Treatments received by patients during the study

Days after diagnosis	Clinical course	Details of the treatment (Chemotherapy regimen)	Nearest point in Figure 2A
0	diagnosis		
5		VCR+Act-D+CPA	
29		VCR+Act-D+CPA	a
49		VCR+Act-D+CPA	
70		VP-16+CPA+THP+CDDP+VCR	b
98		IFM+VP-16+Act-D+VCR	c
126		IFM+VP-16+Act-D+VCR	
154	CR	VP-16+CPA+THP+CDDP+VCR	d
183		VCR+Act-D+CPA	
202	auto-PBSCT	VP-16+L-PAM	
228		RT to site of tumor involvement (50.4Gy)	
277	relapse		e
318		VCR+CPT-11	f
322		RT to clivus (30Gy) and orbit (20Gy)	g
329		VCR+CPT-11	h
343		VCR+CPT-11	j
365		VP-16+CBDCA	l
389		VCR+CPT-11	n
396		VCR+CPT-11	o
415		Act-D+VP-16	

CR, complete remission; auto-PBSCT, autologous peripheral blood stem cell transplantation.
VCR, Vincristine; Act-D, Actinomycin; CPA, Cyclophosphamide; VP-16, Etoposide; THP, Pirarubicin; CDDP, Cisplatin; IFM, Ifosfamide; L-PAM, Melphalan; CPT-11, irinotecan; CBDCA, Carboplatin; RT, radiotherapy.

Supplementary Table S3
Primer sequences used in the study

Name	Sequence	Application	Figure
PAX3(ex5)-f	5 -CGAACCACCTTCACAGCAGAAC-3	RT-PCR (PAX3 fusion, 1st round)	S1
PAX7(ex5)-f	5 -GCCTTTGAGAGGACCCACTACC-3		
FOXO1(ex2)-r	5 -TCTTCTTGGCAGCTCGGCTTCG-3		
FOXO4(ex2)-r	5 -TCAGGGTTCAGCATCCACCAAG-3		
NCOA1(ex11)-r	5 -CTTGAGGAGAAAGCCCACTGTG-3		
NCOA2(ex11)-r	5 -TCCCCATCGTTTGTCCAGTCAG-3		
GAPDHex1-f	5 -GTTCGACAGTCAGCCGCATCTTC-3		
GAPDHex7-r	5 -CAGGGGTGCTAAGCAGTTGGTG-3		
PAX3(ex6)-f	5 -CGTGCAAGATGGAGGAAGCAAG-3	RT-PCR (PAX3 fusion, 2nd round)	
PAX7(ex6)-f	5 -GGCGGCGTTCAACCACCTTCTG-3		
FOXO1(ex2)-r	5 -CTAGGAGATTTCCCGCTCTTGC-3		
FOXO4(ex2)-2-r	5 -GGTGGCCTCGTTGTGAACCTTG-3		
NCOA1(ex10)-r	5 -GTGTGGGCGCTAAGCATTGTCC-3		
NCOA2(ex10)-r	5 -GTGCAGCAACAAGAGTGCCATC-3		
PAX3-g101029r (E-1)	5 -CGGCTTTGAACTTTTCAGCTGCTC-3	Inverse PCR (*EcoR*I digested)	S2
PAX3-g101051f (E-1)	5 -CGGAGGAGTTGAAAAGAATGGATAGC-3		
PAX3-g106957r (E-2)	5 -TCCAATGTACAGGAGAACATAGCTGAC-3		
PAX3-g106981f (E-2)	5 -GGACAAATCAAATGCAACAACCTCG-3		
PAX3-g113697r (E-3)	5 -CAGGAGATGCAATGACCAGAAAGAG-3		
PAX3-g113727f (E-3)	5 -ACCTGGCATTTAATGAGTGTGATCAG-3		

PAX3-g100133r (X-1)	5 -AAGCCCAGAACTAGGATGGAGAAGAC-3	Inverse PCR (*Xba*I digested)	S2
PAX3-g100160f (X-1)	5 -GGTTAAGAAGCTTGCAAACAGTGGC-3		
PAX3-g108029r (X-2)	5 -CATGAGGCTTGGTTTGGTTTCAGG-3		
PAX3-g108065f (X-2)	5 -TCCCCAAAGCAGGCTCTGTAGAAC-3		
PAX3-g112417r (X-3)	5 -CTTCATATGCAGCATACATTTCCATG-3		
PAX3-g112439f (X-3)	5 -GAAGCACACTTGTCTGGCACTCATAC-3		
PGK2-392f	5 - CTGTTGCTGTTGAGCTCAAATCC-3	PCR with DNA (PGK2)	S3
PGK2-508r	5 - CATGAAAGCGCAGGTTCTCCAG-3		
PAX3-g109925f	5 -GAGAACACGGCATCTTTATTGG-3	PCR with cfDNA, DNA (PAX3-FOXO1, 1st)	S3, 2B, 2C, 2E, S4A
FOXO1-g80255r	5 -GGGGTGGTAGAGGAATCTGTAG-3		
PAX3-g110013f	5 -GTAGTTTCTAGCTTTTGGGAGACTG-3	PCR with cfDNA, DNA (PAX3-FOXO1, 2nd),	2B, 2C, 3A 5B, 5D
FOXO1-g80238r	5 -TGTAGGAAAGGAAGCTGGAAAG-3	Quantitative PCR (PAX3-FOXO1)	2D, 3B, 3C, 5A, 5C
PAX3-g109946f	5 -GTTCAGTGTCCCTGGAGTTAGG-3	PCR with cfDNA (PAX3, 1st)	2B, 2C
PAX3-g110142r	5 -CCATGATTGCACCGCTGTACTC-3		
PAX3-g110013f	see abov	PCR with cfDNA (PAX3, 2nd)	
PAX3-g110142r	see abov		
PAX3-g109840f	5 - CCAGCCTACATCAAGTTGCCTG-3	Quantitative PCR (PAX3)	5A, 5C
PAX3-g109949r	5 - CCATACCTAACTCCAGGGACACTG-3		
PGK2-392f	see above	Quantitative PCR (PGK2, internal reference)	2D, 5A, 5C
PGK2-493r	5 - TCTCCAGCAGGATGACTGAACC-3		

Legends to Supplementary Figures

Figure S1

Diagnosis of rhabdomyosarcoma with *PAX3-FOXO1* fusion. (A) Result of ^{18}F-fluoro-2-deoxy-D-glucose positron emission tomography (FDG-PET) scanning at the initial presentation. Significant uptake of FDG was observed at the lymph nodes around both iliac arteries and in bone marrow cavities of the whole body. (B) The morphology of tumor cells in the iliac bone marrow. (C) Detection of *PAX3-FOXO1* fusion gene by reverse transcriptase-polymerase chain reaction (RT-PCR) with bone marrow cells. In the first round of PCR, a mixture of reverse primers for possible partner genes (*FOXO1*, *FOXO4*, *NCOA1*, and *NCOA2*) as well as a forward primer for *PAX3* are used. Amplification of *GAPDH* is used as a positive control for PCR. The second round of PCR is performed with the nested primers for each gene and a forward primer for *PAX3*. The PCR product was purified and directly sequenced. SM, size marker; Pt, patient sample; DW, distilled water.

Figure S2

Isolation of genomic breakpoints of *PAX3-FOXO1* fusion. (A) *Eco*RI and *Xba*I restriction enzyme sites on intron 7 of *PAX3* gene. Location of six pairs of primers for inverse PCR is shown as E-1 to E-3 and X-1 to X-3. Two grey boxes correspond to the location of exon 7 and 8 of *PAX3* gene and short red vertical lines indicate each restriction site. Primers are indicated as small black arrows. Identified genomic breakpoint on intron 7 of *PAX3* gene is shown with red arrow. (B) Results of inverse PCR with these primer pairs. Amplified band from rearranged, non-germline fragment is indicated with a red

arrowhead (lower band of X-2 product). The amplified band was purified and directly sequenced to locate the genomic breakpoint. SM, size marker.

Figure S3

Rhabdomyosarcoma tumor cells in the bone marrow of the patient. (A) Flow cytometry results of the bone marrow cells at relapse. Tumor cells were isolated as abnormal $CD45^-$ $CD56^+$ cells and this population was separated by fluorescence-activated cell sorting (FACS) for genetic analysis. (B) Presence of *PAX3-FOXO1* fusion gene in $CD45^-CD56^+$ tumor cell population. DNA extracted from the sorted populations was subjected to PCR analysis. *PGK2* was used as an endogenous control.

Supplementary Figure S1

A

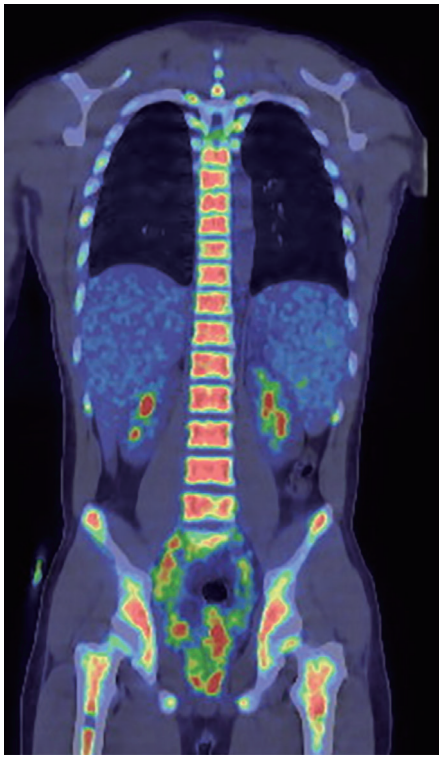

B

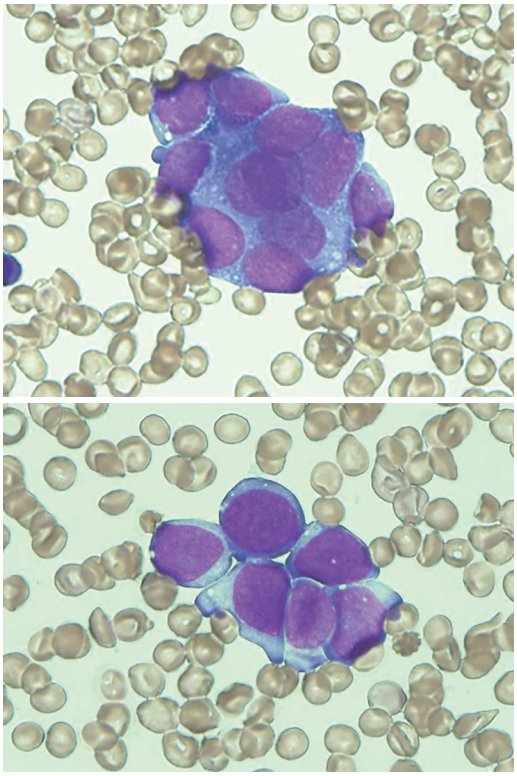

C

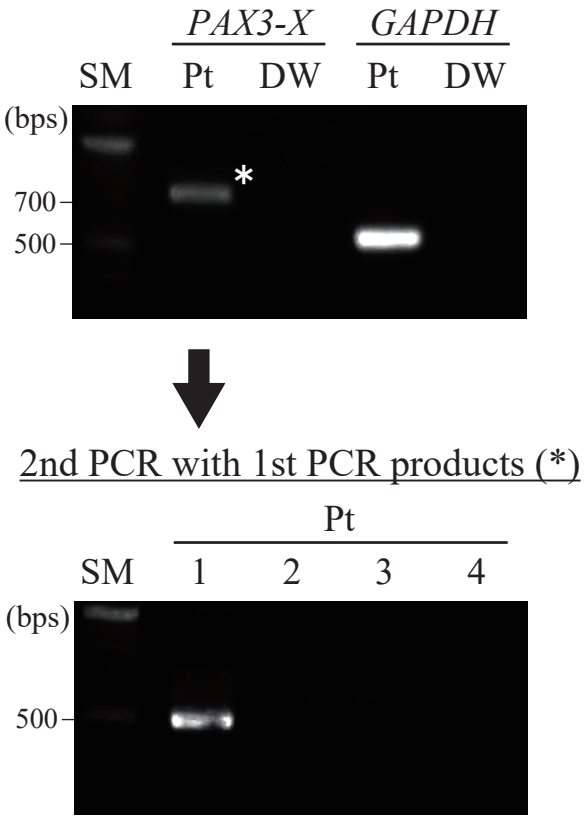

PAX3-X

Forward	Reverse
PAX3(ex5)-f	FOXO1(ex2)-r
	FOXO4(ex2)-r
	NCOA1(ex11)-r
	NCOA2(ex11)-r

	Forward	Reverse
1	PAX3(ex6)-f	FOXO1(ex2)-2-r
2	PAX3(ex6)-f	FOXO4(ex2)-2-r
3	PAX3(ex6)-f	NCOA1(ex10)-r
4	PAX3(ex6)-f	NCOA2(ex10)-r

Supplementary Figure S2

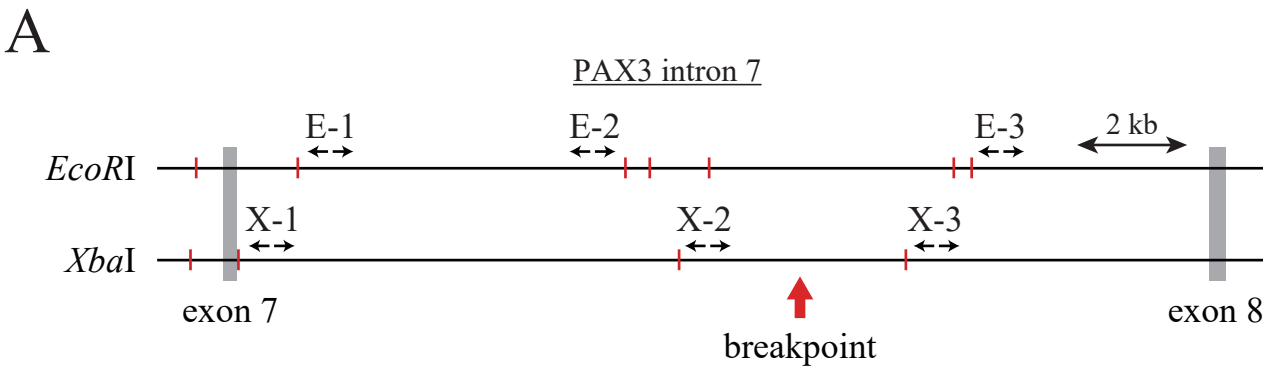

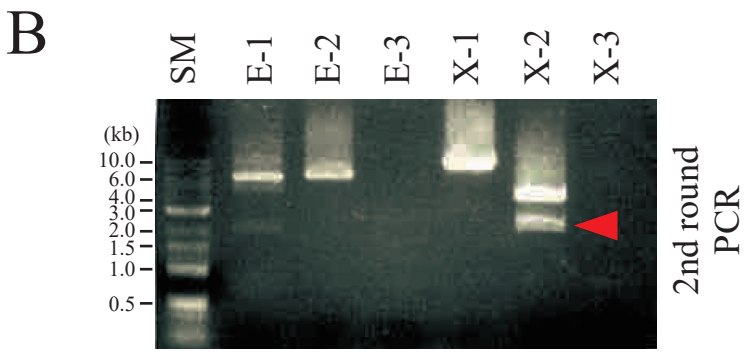

Supplementary Figure S3

A

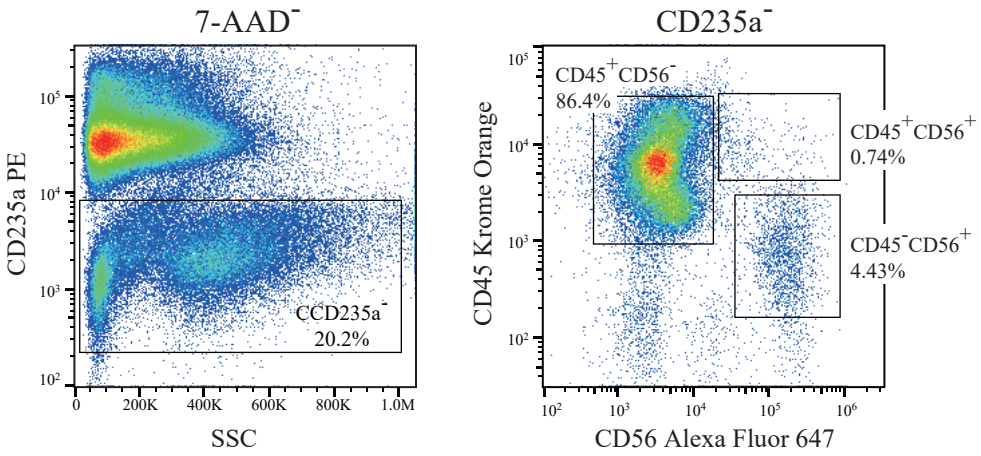

B